Int. J. Heat Mass Transfer. Vol. 23, 861–872

0017-9310/80/0601-0861 $02.00/0

FORCED CONVECTION IN A HORIZONTAL PIPE SUBJECTED TO NONLINEAR EXTERNAL NATURAL CONVECTION AND TO EXTERNAL RADIATION

M. FAGHRI*
Department of Mechanical Engineering, Tehran University of Technology, Tehran, Iran

and

E. M. SPARROW
Department of Mechanical Engineering, University of Minnesota, Minneapolis, MN 55455, U.S.A.

(*Received* 5 *October* 1979 *and in revised form* 29 *November* 1979)

Abstract—An analysis of laminar forced-convection heat-transfer in a horizontal pipe was performed for the case in which the flowing fluid loses heat to the external environment by natural convection and radiation. The temperature difference between the pipe wall and the ambient varies along the pipe. Since the external natural-convection heat-transfer coefficient depends on this temperature difference, it, too, varies along the pipe. The accounting of this variation is a special feature of the analysis. It was found that whereas the pipe Nusselt number is generally insensitive to the variation of the external convection coefficient, a constant-Nusselt-number thermally developed regime does not exist. Radiation tends to lower the pipe Nusselt number, but the maximum effect is only 10%. The wall and bulk temperature distributions are generally more responsive to variable external convection than is the Nusselt number. This responsiveness is diminished when radiation plays an important heat loss role.

NOMENCLATURE

- Bi, Biot number, $\bar{h}r_o/k_i$;
- h, local pipe heat-transfer coefficient, $q/(T_b - T_w)$;
- $\bar{h}_{\Delta Tx}$, circumferential average natural-convection coefficient, based on $(T_w - T_\infty)_x$;
- $\bar{h}$, constant natural-convection coefficient;
- k_i, thermal conductivity of inner fluid;
- k_o, thermal conductivity of outer fluid;
- Nu, pipe Nusselt number, $h(2r_i)/k_i$;
- Pe, Peclet number of inner fluid, $\bar{u}(2r_i)/\alpha$;
- Pr, Prandtl number of outer fluid;
- q, local heat flux based on inside area;
- Ra_x, local Rayleigh number based on $(T_w - T_\infty)_x$, equation (6);
- Ra_1, Rayleigh number based on $(T_1 - T_\infty)$, equation (7);
- r, radial coordinate;
- r_i, inner radius of pipe;
- r_o, outer radius of pipe;
- T, temperature;
- T_b, bulk temperature;
- T_w, wall temperature;
- T_1, inner fluid temperature at inlet;
- T_∞, ambient temperature;
- $\bar{u}$, mean velocity of inner fluid;
- X, dimensionless coordinate $(x/r_i)/Pe$;
- x, axial coordinate.

Greek symbols

- α, thermal diffusivity of inner fluid;
- ε, emissivity of outer pipe surface;
- η, dimensionless coordinate, r/r_i;
- θ, dimensionless temperature, $(T - T_\infty)/(T_1 - T_\infty)$;
- θ_b, dimensionless bulk temperature, $(T_b - T_\infty)/(T_1 - T_\infty)$;
- θ_w, dimensionless wall temperature, $(T_w - T_\infty)/(T_1 - T_\infty)$;
- σ, Stefan–Boltzmann constant;
- ϕ, function of Prandtl number, equation (5a).

1. INTRODUCTION

MOST ANALYSES of forced-convection heat transfer in pipes are predicated on the assumption that a great deal of information is known at the pipe wall. In this connection, it may be noted that prescribed wall temperature and prescribed wall heat flux are the most common boundary conditions for pipe-flow heat-transfer analysis. If there is convective heat exchange between the outer surface of the pipe and a fluid environment, it is assumed that the value of the external heat-transfer coefficient is known *a priori* and is normally taken to be a constant.

In reality, the amount of *a priori* information available is frequently less than that which is employed in pipe-flow heat-transfer analyses. For example, consider a fluid flowing through a horizontal pipe which loses heat by natural convection from its outer surface to a large external fluid environment. If the temperature of the internal flow is higher than that of the

* Work performed when the author was an adjunct associate professor at the University of Minnesota.

environment, both the bulk and wall temperatures will decrease in the flow direction. Since the external natural convection is controlled by the difference between the local wall temperature and the ambient temperature, the external heat-transfer coefficient will also decrease in the flow direction. However, the axial distribution of the wall temperature is not known *a priori*; rather, it is a result of the interaction between heat-transfer processes internal and external to the pipe. Therefore, in this situation, the external heat-transfer coefficient is not known *a priori*.

The foregoing discussion identifies one of the foci of the present research, namely, pipe-flow problems with interactively determined thermal boundary conditions. Specific consideration is given to the very problem discussed above. A laminar, forced-convection flow enters a horizontal pipe which is situated in an extensive fluid environment at temperature T_∞. Heat loss occurs at the outer surface of the pipe by natural convection. The resulting axial variation of the wall temperature affects both the heat-transfer characteristics of the pipe flow and of the external natural convection. In the analysis presented here, the energy-conservation equation for the pipe flow is solved subject to a wall-boundary condition which accommodates the interactively determined variations of the natural convection heat-transfer coefficient.

If the fluid external to the pipe is a gas such as air, then radiative transfer may supplement the natural-convection heat loss from the outside surface of the pipe. The extent of the radiative contribution depends on the emissivity of the surface and on the temperature level. Even for moderate temperatures, the radiative transfer will equal that for natural convection when the emissivity is ~ 1. Therefore, when the external environment is a gas, a realistic thermal boundary condition for the pipe-flow problem should account for both natural convection and radiation.

The second focus of the present research is to solve the forced-convection pipe flow subject to simultaneous external natural-convection and radiation. The solutions involving radiative transfer will incorporate the interactively determined variations of the natural convection heat-transfer coefficient.

An appraisal of the governing equations reveals a superabundance of prescribable parameters. In the no-radiation case, there are three prescribable parameters, whereas with radiation there are a total of five parameters. In view of the lengthy numerical computations that are required for each case, the parameter values were selected to be representative but not necessarily complete.

In addition to the solutions discussed above (i.e. characterized by variable external convection without and with radiation), it was deemed appropriate, for comparison purposes, to obtain results for the case where the natural-convection coefficient is constant and prescribed *a priori*. These supplementary solutions will be designated as the constant Biot number solutions, and they were obtained both without and with radiation.

A survey of the literature on forced-convection pipe flow did not reveal any prior work on either of the main lines of the present research. There is, of course, related work which forms the background for the new effects that were investigated here. The problem of laminar pipe flow with a constant, *a priori* prescribed external heat-transfer coefficient has been solved by a number of investigators using a variety of solution methods, for example [1–5]. Laminar pipe flow with external radiation transfer (without natural convection) has also been analyzed and solutions obtained by using several different approaches [6–9].

2. ANALYSIS

2.1. *Mathematical formulation*

Consider a laminar fluid flow in a horizontal circular pipe in which x is the axial coordinate and r is the radial coordinate; the inner and outer radii of the pipe wall are r_i and r_o, respectively. At $x = 0$, the fluid temperature is uniform and equal to T_1. For $x > 0$, the outer surface of the pipe is exposed to a fluid environment where the temperature is T_∞ ($T_\infty \neq T_1$). The environment is free of fluid motions except for the natural convection induced by the presence of the pipe. If the fluid is a transparent gas (e.g. air), it is enclosed by walls that are also at temperature T_∞.

With regard to the velocity field in the pipe, it is envisioned that there is a hydrodynamic-development section upstream of $x = 0$. Therefore, in the heat-transfer section, the velocity profile is fully developed and equal to the Poiseuille parabola.

The pipe wall is assumed to be highly conducting so that its temperature is circumferentially uniform at any cross section; furthermore, the temperature drop across the thickness of the wall is taken to be negligible. Generalization of the analysis to include radial temperature variations across the wall thickness can readily be accomplished, but this would add still another parameter to the already excessive number that appear in the problem. The accounting of circumferential variations would change the entire nature of the solution task and is beyond the scope of the present research.

The starting point for the analysis is the energy conservation equation for the pipe flow. By introduction of dimensionless variables

$$X = \frac{x/r_i}{Pe}, \quad \eta = \frac{r}{r_i}, \quad \theta = \frac{T - T_\infty}{T_1 - T_\infty}, \quad Pe = \frac{\bar{u}(2r_i)}{\alpha} \tag{1}$$

the energy equation becomes

$$(1 - \eta^2)\frac{\partial \theta}{\partial X} = \frac{1}{\eta}\frac{\partial}{\partial \eta}\left(\eta \frac{\partial \theta}{\partial \eta}\right). \tag{2}$$

Note that axial conduction has not been included because low Peclet-number flows are not being considered.

The pipe-wall boundary conditions will now be examined, and attention will first be focused on external natural convection, without radiation. Since the wall temperature T_w is circumferentially uniform, the external heat-transfer coefficient that is needed for the formulation of the boundary condition is the circumferential-average value. This coefficient will be denoted by $\bar{h}_{\Delta Tx}$ to underscore the fact that it depends on the local wall-to-ambient temperature difference at x. Then, at any axial station x,

$$-k_i r_i(\partial T/\partial r)_{r_i} = \bar{h}_{\Delta Tx} r_o (T_w - T_\infty) \tag{3}$$

or, in terms of the dimensionless variables of (1)

$$-(\partial\theta/\partial\eta)_{\eta=1} = [\bar{h}_{\Delta Tx}(2r_o)/k_o](k_o/k_i)\theta_w/2. \tag{4}$$

In this equation, k_i and k_o respectively denote the thermal conductivities of the internal and external fluids.

The quantity in brackets in equation (4) is the circumferential-average natural convection Nusselt number corresponding to a yet undetermined temperature difference $(T_w - T_\infty)_x$. At each axial station x, this Nusselt number can be associated with that for an isothermal cylinder with a uniform temperature difference equal to $(T_w - T_\infty)_x$. From a consideration of the available information for natural-convection heat transfer about an isothermal horizontal cylinder, the recent correlation of Churchill and Chu [10] appears to be the most encompassing. That correlation is especially useful because it covers, with a single algebraic relationship, Rayleigh numbers between 10^{-6} and 10^9 and all Prandtl numbers. The correlating equation is

$$\overline{Nu} = 0.36 + 0.518Ra^{1/4}/\phi(Pr), \tag{5}$$

$$\phi(Pr) = [1 + (0.559/Pr)^{9/16}]^{4/9}. \tag{5a}$$

It should be noted that $\phi(Pr)$ varies only moderately with Pr, ranging from 1.32 for $Pr = 0.7$ to 1.0 as $Pr \to \infty$ (very viscous oils).

In accordance with the foregoing discussion, equation (5) is to be applied locally in the evaluation of the Nusselt number $\bar{h}_{\Delta Tx}(2r_o)/k_o$ that appears on the RHS of the boundary condition (4). Correspondingly, the Rayleigh number is interpreted as

$$Ra_x = g\beta(T_w - T_\infty)_x(2r_o)^3/\alpha\nu \tag{6}$$

where all properties refer to the external fluid. If the dimensionless temperature θ is introduced, Ra_x becomes

$$Ra_x = \theta_{wx}Ra_1, \quad Ra_1 = g\beta(T_1 - T_\infty)(2r_o)^3/\alpha\nu. \tag{7}$$

The Rayleigh number Ra_1 corresponds to the overall temperature difference $(T_1 - T_\infty)$ at the start of the heat-transfer section. This is the only temperature difference which can be identified prior to the solution of the problem since the wall and bulk temperatures vary and are not known in advance. Therefore, Ra_1, being known *a priori*, can realistically serve as one of the prescribable parameters.

Upon returning to the boundary condition (4) with inputs from equations (5) and (7), there follows

$$-(\partial\theta/\partial\eta)_{\eta=1} = \tfrac{1}{2}[0.36 + 0.518Ra_1^{1/4}\theta_{wx}^{1/4}/\phi](k_o/k_i)\theta_{wx} \tag{8}$$

Equation (8) is the final form of the boundary condition for the pipe-flow problem when the external heat loss is by natural convection. The novel feature of the formulation can be identified by examination of this equation. Since θ_{wx} decreases with x, so does $\theta_{wx}^{1/4}$ and, as a consequence, the natural convection Nusselt number [square bracketed terms of equation (8)] decreases with x, giving rise to an increase of the thermal resistance. It is in the accounting of this effect that the present analysis differs from prior studies of pipe flows with an external convective boundary condition.

Further examination of the governing equations (2) and (8) reveals the presence of three prescribable physical parameters

$$Ra_1, \quad k_o/k_i, \quad Pr. \tag{9}$$

The number of computational parameters can be reduced by noting that the Rayleigh and Prandtl numbers are grouped together in equation (8) in the ratio $Ra_1^{1/4}/\phi$.

When radiative transfer takes place between the outer surface and the environment, then an additional term has to be appended to the RHS of equation (8). If the pipe is situated in a space whose walls are at T_∞ and if the wall area is much larger than that of the pipe surface, then the radiation filling the space is black radiation corresponding to T_∞. Furthermore, if the surface of the pipe is gray with an emissivity ε then the local radiative heat loss at x, per unit surface area, is

$$\sigma\varepsilon(T_{wx}^4 - T_\infty^4). \tag{10}$$

When this expression is incorporated into the local heat balance at the wall, there follows*

$$-(\partial\theta/\partial\eta)_{\eta=1} = \text{RHS}(8) + \frac{\sigma\varepsilon r_o}{k_i}\,\frac{T_{wx}^4 - T_\infty^4}{T_1 - T_\infty}. \tag{11}$$

Upon introduction of the dimensionless temperature θ into equation (11), there is obtained, after rearrangement

$$-(\partial\theta/\partial\eta)_{\eta=1} = \text{RHS}(8) + \left(\frac{k_o}{k_i}\right)\left[\frac{\varepsilon\sigma T_\infty^3 r_o}{k_o}\right] \times \frac{[\theta_{wx}(T_1/T_\infty - 1) + 1]^4 - 1}{T_1/T_\infty - 1}. \tag{12}$$

Examination of equation (12) reveals that the accounting of radiative transfer has added two additional parameters, namely

$$\varepsilon\sigma T_\infty^3 r_o/k_o, \quad T_1/T_\infty. \tag{13}$$

* With RHS(8) denoting the right-hand side of equation (8).

If $\varepsilon\sigma T_s^3$ is regarded as a radiation heat-transfer coefficient, then $\varepsilon\sigma T_s^3 r_o/k_o$ has the appearance of a radiation Nusselt number. The larger the value of this parameter, the greater the strength of the radiative transfer. The radiation contribution is also strengthened by increasing values of T_1/T_s, provided that θ_{wx} is not too small.

Equation (2) along with either of the pipe-wall energy balances (8) or (12) constitute the governing equations for the pipe-flow problem with interactively determined thermal-boundary conditions. To these is added the initial condition $\theta = 0$ at $x = 0$. The solution methodology for these equations will be described shortly.

2.2. *Simplified external-convection model*

For comparison with the present results, solutions were also carried out for a simpler model of the external natural convection, namely, for the case in which the external-convection coefficient is uniform and known *a priori*. In implementing such a model, consideration has to be given to how the convection coefficient, which depends on $T_w - T_s$, is to be selected. As noted earlier, $T_w - T_s$ varies with x, beginning with an initial value $T_1 - T_s$ at $x = 0$ and decreasing (i.e. when $T_1 > T_s$) to an *a priori* unknown final value at the downstream end of the pipe. Since $T_1 - T_s$ is the only wall-to-fluid temperature difference that is known in advance, it will be used to evaluate the given constant value of h, which will be denoted by $\bar{h}$.

For convective heat loss corresponding to the uniform and known external coefficient $\bar{h}$, the pipe-wall heat balance becomes

$$-(\partial\theta/\partial\eta)_{\eta=1} = (\bar{h}r_o/k_i)\theta_{wx} \equiv Bi\,\theta_{wx} \qquad (14)$$

which contains only one parameter, the Biot number Bi. When radiation supplements natural convection, equation (14) becomes

$$-(\partial\theta/\partial\eta)_{\eta=1} = Bi\theta_{wx} + \left[\frac{\varepsilon\sigma T_s^3 r_o}{k_i}\right] \times \frac{[\theta_{wx}(T_1/T_s - 1) + 1]^4 - 1}{T_1/T_s - 1} \qquad (15)$$

in which three prescribable parameters are in evidence.

To compare the results from the constant Biot-number model with those for the more general natural-convection model formulated earlier, Bi is evaluated from

$$Bi = \tfrac{1}{2}(0.36 + 0.518Ra_1^{1/4}/\phi)(k_o/k_i) \qquad (16)$$

and the radiation parameter of equation (15) follows from

$$\varepsilon\sigma T_s^3 r_o/k_i = (\varepsilon\sigma T_s^3 r_o/k_o)(k_o/k_i). \qquad (17)$$

The values of Ra_1, Pr, k_o/k_i, and $\varepsilon\sigma T_s^3 r_o/k_o$ which (along with T_1/T_s) define a given case for the generalized problem were introduced into equations (16) and (17) to fix the comparison case for the simplified model.

2.3. *Solution methodology*

The numerical solutions were carried out by adapting the Patankar–Spalding (P–S) method to the governing equations of the present problem. Two of the adaptations will be discussed here. It should be noted that the P–S method is an implicit marching procedure which is formulated to solve a set of *N linear* algebraic equations at each forward step. Neither the convective nor the radiative boundary conditions of the present problem are linear, so that some adaptation is needed. Provided that a sufficiently small forward step size ΔX is employed, the boundary conditions can be locally linearized in a simple fashion without significant loss of accuracy. For example, if computations are being performed at an axial station X_j, then the θ_{wx} that appears in the square brackets of equation (8) can be evaluated using the known value (i.e. known from the preceding calculations) of θ_w at X_{j-1}. Although exceedingly small steps were employed in the present calculations, it was decided to employ a more refined local linearization to ensure that no perceptible error would occur.

To this end, let $G(\theta_{wx})$ denote any one of the expressions which appear on the RHSs of equations (8), (12), or (15). Also, for compactness, let θ_w at X_j be θ_j, and θ_w at X_{j-1} be θ_{j-1}. Then, at X_j, the boundary condition can be approximated as

$$-(\partial\theta/\partial\eta)_{\eta=1} = G(\theta_{j-1}) + G'(\theta_{j-1})(\theta_j - \theta_{j-1}) \qquad (18)$$

where $G' = \partial G/\partial\theta_{wx}$ represents the algebraic expression obtained by differentiating G with respect to θ_{wx}. Since θ_{j-1} is known from the calculations at the prior step, equation (18) is a linear form which is acceptable to the P–S method. By making $X_j - X_{j-1}$ sufficiently small, the error associated with the local linearization can be made altogether negligible, as was verified in the computations.

The other adaptation had to do with 'tuning' the program with regard to both step size and deployment of the grid points. To this end, it was found useful to make comparisons with the eigenvalue solution of [2] for constant Biot number and no radiation. With only ten eigenvalues available, that solution is limited to the downstream portion of the pipe. In that region, the local Nusselt numbers from the present solutions agreed to within 0.01% with those from the eigenvalue solutions. The final computer runs were made with 200 points in the cross section and at about 10 000 axial stations.

3. RESULTS AND DISCUSSION

The cases for which numerical solutions were carried out are listed in Table 1. In the table, cases A, B,..., I refer to situations where the external natural convection is determined interactively, whereas A', B',..., I' are the corresponding constant Biot-number comparison cases. Solutions accounting for natural-convection heat loss were performed for each of the tabulated cases, and solutions involving simultaneous natural convection and radiation were obtained for the

Table 1. Parameter values for the computations

Case	k_o/k_i	$Ra_1^{1/4}/\phi$	Bi	$(k_o/k_i)^*$
A	1	2.4		
A′			0.80	1
B	1	7.5		
B′			2.1	1
C	1	13.4		
C′			3.7	1
D	1	23.9		
D′			6.4	1
E	1	42.5		
E′			11.2	1
F	0.05	13.4		
F′			0.18	0.05
G	0.2	13.4		
G′			0.73	0.2
H	5	15.9		
H′			21.5	5
I	20	15.9		
I′			85.8	20

Radiation cases $T_1/T_\infty = 1.25$, $\varepsilon\sigma T_\infty^3 r_o/k_o = 1$.
* For input to equation (17) only.

majority of these cases, as will be seen shortly. The tabulated values of $Ra_1^{1/4}/\phi$ are not simple integer-type numbers. This is because the computations were originally performed for specified values of Ra_1 and Pr, and the group $Ra_1^{1/4}/\phi$ was subsequently evaluated.

Results will be presented for the axial distributions of three quantities: the local pipe-flow Nusselt number Nu, the local bulk temperature $\theta_b = (T_b - T_\infty)/(T_1 - T_\infty)$, and the local wall temperature $\theta_w = (T_w - T_\infty)/(T_1 - T_\infty)$. The local Nusselt number is defined as

$$Nu = h(2r_i)/k_i, \quad h = q/(T_b - T_w) \qquad (19)$$

where q is the local heat flux per unit inside pipe-wall area.

The reason for presenting the wall- and bulk-temperature distributions in addition to the Nusselt number is apparent from equation (19). Since q, T_w, and T_b are all unknown at any axial station, a knowledge of the Nusselt number (or h) is insufficient to determine any of these quantities. Rather, two among q, T_w, and T_b have to be given in addition to Nu.

3.1. *Nusselt number distributions*

Axial distributions of the local pipe-flow Nusselt number are presented in Figs. 1–3. Figure 1 is for $k_o/k_i = 1$, that is, the same fluid inside and outside the pipe. Figures 2 and 3 are, respectively, for cases where $k_o/k_i < 1$ and $k_o/k_i > 1$. Each figure conveys results for numerous cases and it is, therefore, appropriate to describe the structure of the figures.

Consider, for example, Fig. 1. The main part of the figure gives results at axial positions between X of 0.002 and 1, while the inset at the upper right extends the results back to $X = 0.0004$. The curves are grouped according to the designations in Table 1, e.g. A,A′, B,B′, etc. with a given unprimed case being paired with the corresponding primed case. At the lower left, a legend describes the characteristics of each curve. The designation Ra_x means that the external natural convection is determined interactively, while Bi means that the Biot number is prescribed and constant; RAD and W/O RAD are self explanatory. Curves E,E′ are referred to the outer (leftmost) left-hand ordinate, while curves B,B′ refer to the inner left-hand ordinate; curves A,A′ are read from the right-hand ordinate. A similar structural description also applies to Figs. 2 and 3.

The major issues to be examined in Figs. 1–3 are: (1) the response of the pipe Nusselt number to the axial

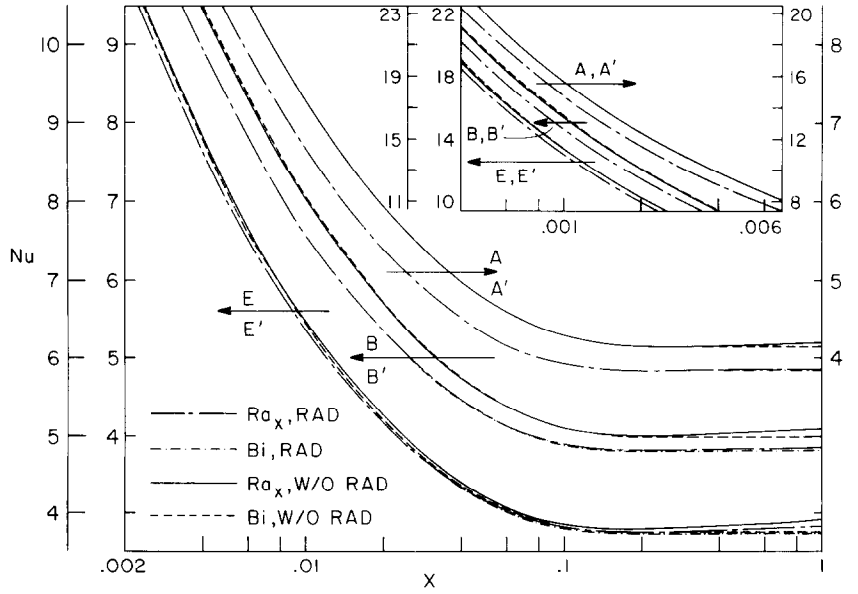

FIG. 1. Local Nusselt-number distributions for cases A and A′, B and B′, and E and E′ (all with $k_o/k_i = 1$), without and with radiation.

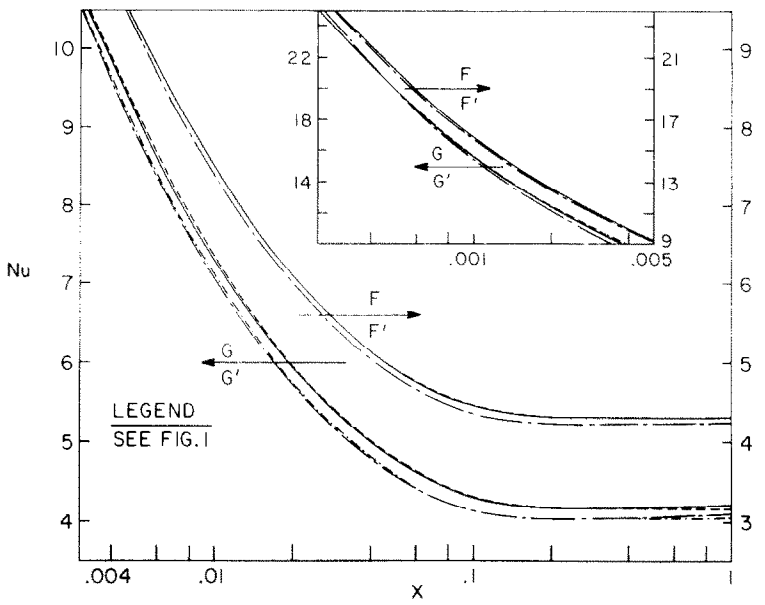

FIG. 2. Local Nusselt-number distributions for cases F and F', and G and G' (all with $k_o/k_i < 1$), without and with radiation.

variations of the interactively determined external natural convection, (2) the effect of external radiative transfer, (3) the existence or nonexistence of a thermally developed regime in the presence of external non-linear heat transfer, either by natural convection or radiation, (4) the effect of k_o/k_i, $Ra_1^{1/4}/\phi$, and Bi on the magnitude of Nu.

Examination of Figs. 1–3 reveals that the corresponding Ra_x and Bi Nusselt-number distributions are essentially identical, except in the far downstream region for certain selected cases. The Nusselt number is, therefore, insensitive to whether the external convection coefficient remains constant at its initial (i.e. $x = 0$) value or decreases with x as $T_w - T_\infty$ decreases. This outcome is especially noteworthy since, as will be seen shortly, the ingredients which make up h do respond to the details of the external convection.

An even more convincing demonstration of the forgiving nature of Nu (or h) to the external transfer may be seen by examining the effects of radiation in Figs. 1–3. It is seen that there are deviations between the with-radiation and no-radiation cases in the lower

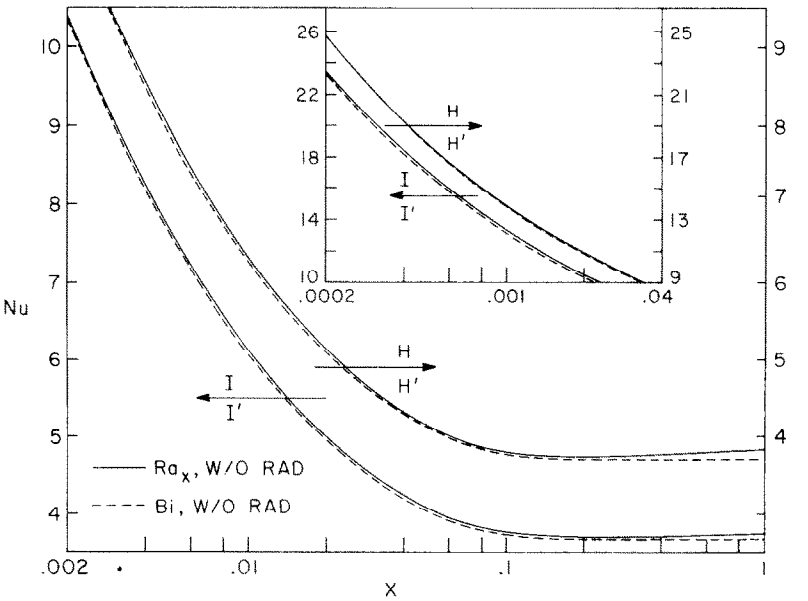

FIG. 3. Local Nusselt-number distributions for cases H and H', and I and I' (all with $k_o/k_i > 1$), without radiation.

ranges of the quantities $Ra_1^{1/4}/\phi$ and $Bi(k_o/k_i)$. The extreme deviation between the results is about 10% (cases A or A'). This deviation will be shown to be moderate compared with the impact of radiation on T_w or T_b.

Thus, from the foregoing, it appears that because of compensating variations among its component parts, the heat-transfer coefficient is relatively insensitive to the details of the external boundary condition.

There are a number of thermal boundary conditions which give rise to a thermally-developed regime in which Nu is independent of x, and all of these appear to be linear [11]. The present solutions provide an opportunity of examining the possible presence of a constant Nusselt number regime when the boundary conditions are non-linear.

Inspection of the downstream (large X) portion of Figs. 1–3 shows that for non-linear natural convection, the curves (i.e. the Ra_x curves) tend to attain a shallow minimum and then rise very gradually. For the largest X of the graphs, the deviations due to the rise are very small—just a few per cent. Interestingly enough, the presence of radiation does not, in itself, give rise to the just mentioned behavior. Indeed, for radiation and linear natural convection, the plotted curves are flat, although the higher significant figures of the computer print-outs show a tendency for Nu to increase with X. The existence of an apparent thermally developed regime in the presence of radiation is a major surprise.

The effect of the parameters on the magnitude of Nu will now be discussed. In [11], for the case of Bi = constant and thermally-developed conditions, it was shown that Nu decreases with increasing Bi, the overall decrease of Nu being about 19% as Bi ranges from 0 to ∞. Inspection of Figs. 1–3 reveals a similar trend at any given axial station in the development regime; that is, Nu decreases as either $(k_o/k_i)(Ra_1^{1/4}/\phi)$ or Bi increase. The range of the decrease is within the aforementioned 19%. Radiation, which comes to greater prominence when $Ra_1^{1/4}/\phi$ or $Bi/(k_o/k_i)$ is small, tends to decrease the Nusselt number, but by 10% at most.

3.2. *Wall and bulk temperature distributions*

The results for the axial distributions of the wall and bulk temperature are presented in Figs. 4–10. The initial discussion will be focused on Figs. 4–6, which show results for $k_o/k_i = 1$ (same inner and outer fluid), respectively corresponding to cases A and A', B and B', and E and E'. When radiation is not taken into account, these results pertain to any fluid provided that the parametric values of $Ra_1^{1/4}/\phi$ or Bi are appropriate. The no-radiation results of Figs. 4–6 can be so interpreted. On the other hand, if comparisons are to be made between no-radiation and with-radiation results for otherwise identical conditions, then the external fluid must be a transparent gas. For concreteness in the discussion of radiative effects, it will be assumed that the outside fluid is air ($Pr = 0.7$) and, correspondingly, for Figs. 4–6, the inner fluid is also air.

Figures 4–6 have a common structure. In each figure, the θ_w and θ_b curves for a specified non-radiative situation are plotted in the upper portion, and the θ_w and θ_b curves for the corresponding with-radiation situation are shown in the lower portion. The upper curves are referred to the right-hand ordinate, while the lower curves are referred to the left-hand ordinate. Solid and dashed lines are respectively employed to denote variable external natural convection and uniform external natural convection. For the interpretation of the figures, it should be noted that the value of $Ra_1^{1/4}/\phi$ and Bi are relatively small for Fig.

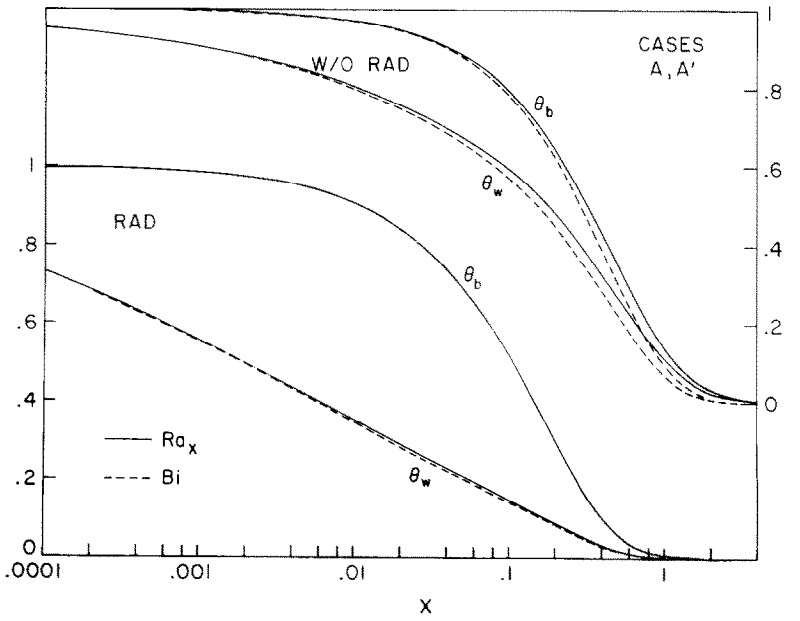

FIG. 4. Wall- and bulk-temperature distributions for cases A and A', without and with radiation.

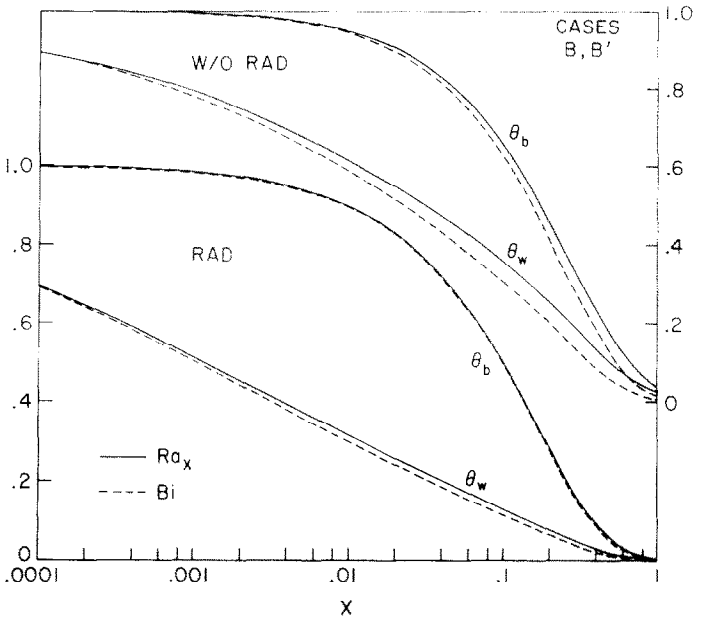

FIG. 5. Wall- and bulk-temperature distributions for cases B and B', without and with radiation.

4 and increase successively in Figs. 5 and 6.

First considering Fig. 4 and focusing on the no-radiation case, it is seen that both the bulk and wall temperatures decrease rather slowly with X and that the difference between θ_b and θ_w is not very large. This is due to the relatively low rates of heat transfer associated with the weak external convection. When radiation is brought into play (lower diagram of Fig. 4), it provides a much more effective heat-loss path than that provided by the external convection. As a consequence, both the wall- and bulk-temperature curves drop off more rapidly, especially the former.

The importance of variable external convection is affected by the presence or absence of radiation. Without radiation, the results show some sensitivity to variable external convection, but when radiation acts, the external convection becomes of lesser importance, as does its variability.

When the external convection is stronger (Fig. 5), the aforementioned trends are modified. In the no-radiation case, the wall and bulk temperatures drop off more rapidly than before. Furthermore, the effect of variable external convection is heightened, especially with regard to the wall temperature. The augmented

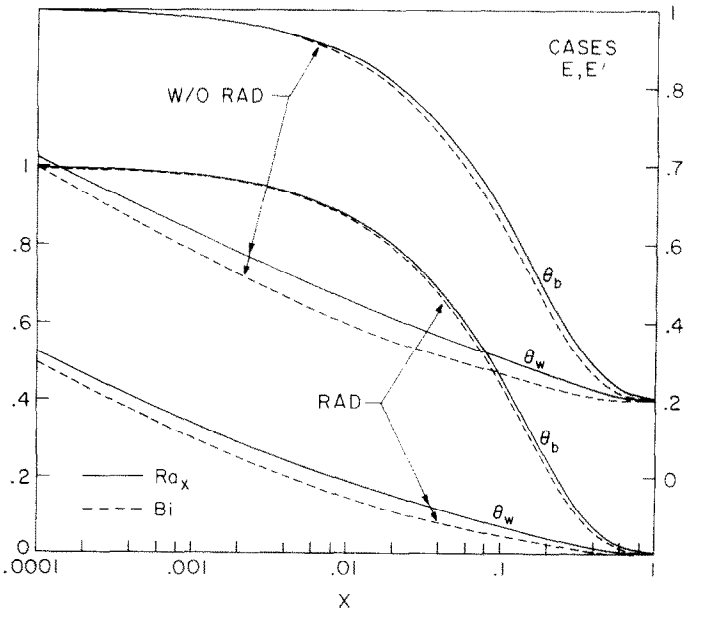

FIG. 6. Wall- and bulk-temperature distributions for cases E and E', without and with radiation.

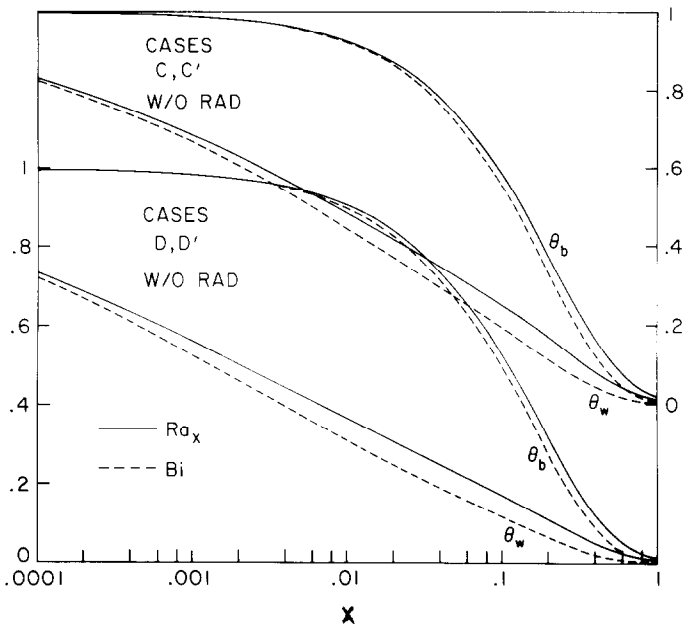

FIG. 7. Wall- and bulk-temperature distributions for cases C and C', and D and D', without radiation.

role of variable external convection can be understood by examining the square bracket of equation (8) and noting that the role of the constant term is washed out as $Ra_1^{1/4}/\phi$ is increased. When radiation is involved, the heat-transfer rates increase, causing more rapid changes in θ_w and θ_b; as before, the effect of variable external convection is muted.

Figure 6 corresponds to a case of relatively strong external convection. The no-radiation situation shows rapid drop-offs in θ_w and θ_b as well as moderately important influences of variable external convection, especially with regards θ_w. When radiation is brought into play, its effect is much less than at lower values of $Ra_1^{1/4}/\phi$ or Bi.

The presentation of results for the case of $k_o/k_i = 1$ (same inner and outer fluid) is completed by Fig. 7. In this figure, θ_w and θ_b distributions are plotted for cases C and C' and for cases D and D', all for external natural convection without radiation. The trends in evidence in this figure are in agreement with those discussed in the foregoing paragraphs and need no elaboration. Figure 7 is included in order to provide information at a sufficient number of $Ra_1^{1/4}/\phi$ values to permit accurate interpolations.

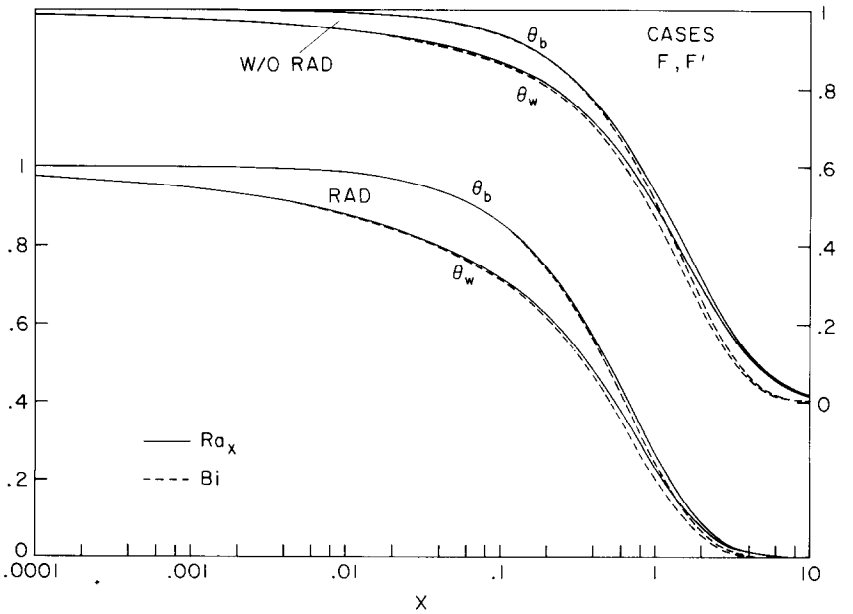

FIG. 8. Wall- and bulk-temperature distributions for cases F and F', without and with radiation.

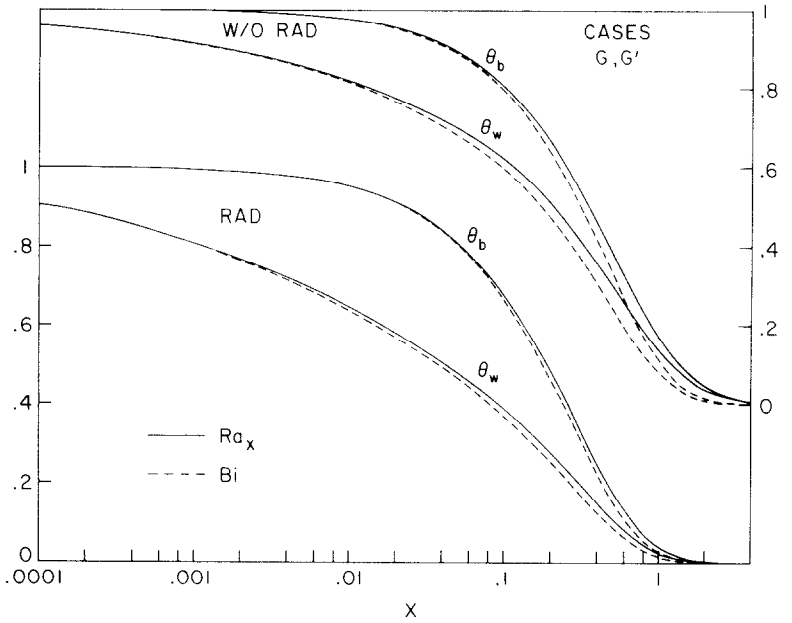

FIG. 9. Wall- and bulk-temperature distributions for cases G and G', without and with radiation.

Attention is next turned to situations where $k_o/k_i \neq 1$. Consideration is first given to cases F,F' and G,G', which are characterized by $k_o/k_i < 0$. The no-radiation results for these cases are applicable to any fluid combinations which match the parameter values, but for discussing the radiation results it is convenient to think of cases F,F' as water inside–air outside and of cases G,G' as oil inside–air outside.

The wall- and bulk-temperature results for these cases are presented in Figs. 8 and 9 using a format identical to that of Figs. 4–6. The general trends in these figures are the same as those of the earlier figures, but certain details are worth noting. Owing to the relatively low values of (k_o/k_i) $(Ra_1^{1/4}/\phi)$ or of Bi, the external natural convection is quite weak and the rate of heat loss is correspondingly low when radiation does not participate. Also, the results are moderately sensitive to variable external convection. When radiation acts, the heat-transfer rate is appreciably augmented as witnessed by the more rapid drop-off of the curves and the diminished sensitivity to variable external convection.

Results for $k_o/k_i > 1$ comprise the final item in the presentation of results—specifically, cases H and H'

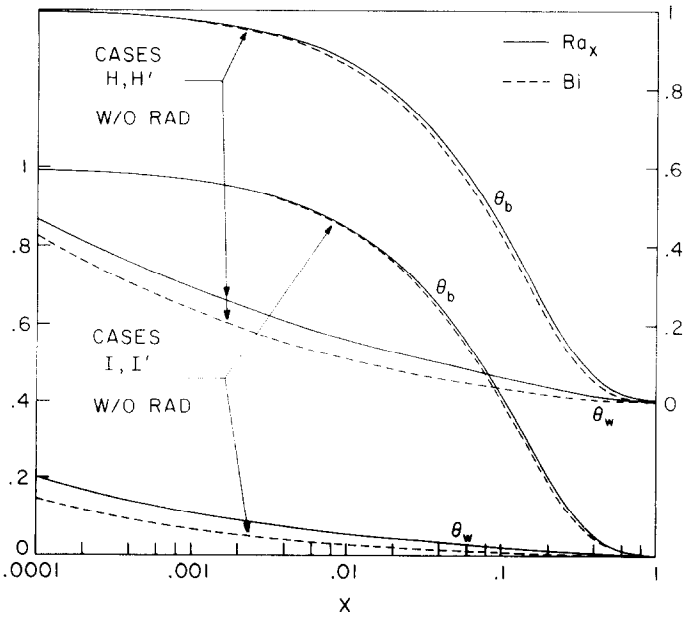

FIG. 10. Wall- and bulk-temperature distributions for cases H and H', and I and I', without radiation.

and cases I and I′ of Table 1. These cases were selected to characterize the presence of a liquid external to the tube with a conductivity much higher than that of the internal fluid. Appropriately high values of (k_o/k_i) $(Ra_1^{1/4}/\phi)$ and of Bi can be noted in Table 1. The main features of the results shown in Fig. 10 are the evidences of the high rates of heat transfer and low external thermal resistance. The wall and bulk temperatures diminish rapidly, and the wall temperature takes on values that do not differ much from those of the ambient. Thus, as an approximation, cases such as these can be treated as if the wall temperature were uniform and equal to T_∞. The variability of the external convection has little effect on the heat transfer rates (i.e. on θ_b) because the major resistance to heat transfer is in the fluid flowing within the tube.

4. CONCLUDING REMARKS

One of the main findings that has emerged from the presentation of results is the insensitivity of the pipe Nusselt number to nonlinear external natural convection or to radiation. The Nusselt numbers are essentially the same regardless of whether the external-convection coefficient remains constant at its $x = 0$ value or varies with x as $T_w - T_\infty$ changes. When the external convection is weak, radiation tends to decrease the Nusselt number slightly, with the change being 10%, at most.

The nonlinear external convection appears to preclude a constant Nusselt number regime, as is normally encountered in a thermally developed pipe flow. Rather, in the downstream portion of the pipe, the Nusselt number curve attains a shallow minimum and then rises slowly. The extent of the rise is, at most, only a few per cent at the farthest downstream position examined. The magnitudes of the Nusselt number are moderately affected by changes in either (k_o/k_i) $(Ra_1^{1/4}/\phi)$ or Bi, decreasing as these quantities increase.

The wall- and bulk-temperature distributions are generally more responsive to variable external convection than is the Nusselt number. The distribution curves for the variable-convection case drop off more slowly with x than do those for the corresponding constant Biot number case. Radiation has two influences on the distributions. First, when radiation is present, the wall and bulk temperatures drop off more rapidly than when there is negligible radiation. Second, radiation tends to diminish the sensitivity of the results to variable natural convection. The role of radiation is accentuated when the external convection is relatively weak.

Acknowledgement—This research was performed, in part, under the auspices of the National Science Foundation (ENG-7518141 A01) and with the support (to M. F.) of the Iranian Ministry of Education.

REFERENCES

1. S. Sideman, D. Luss and R. E. Peck, Heat transfer in laminar flow in circular and flat conduits with constant surface resistance, *Appl. Scient. Res.* **A14**, 157–171 (1964–1965).
2. C. J. Hsu, Exact solution to entry-region laminar heat transfer with axial conduction and the boundary condition of the third kind, *Chem. Engng Sci.* **23**, 457–468 (1968).
3. A. A. McKillop, J. C. Harper and H. J. Bader, Heat transfer in entrance-region flow with external resistance, *Int. J. Heat Mass Transfer* **14**, 863–866 (1971).
4. C. J. Hsu, Laminar flow heat transfer in circular or parallel-plate channels with internal heat generation and the boundary condition of the third kind, *J. Chinese Inst. Chem. Engrs.* **2**, 85–100 (1971).
5. V. Javeri, Simultaneous development of the laminar velocity and temperature fields in a circular duct for the temperature boundary conditions of the third kind. *Int. J. Heat Mass Transfer* **19**, 943–949 (1976).
6. J. C. Chen, Laminar heat transfer in tube with nonlinear radiant heat flux boundary condition, *Int. J. Heat Mass Transfer* **9**, 433–440 (1966).
7. B. I. Dussan and T. F. Irvine, Jr., Laminar heat transfer in a round tube with radiating heat flux at the outer wall, *Proceedings of the Third International Heat Transfer Conference*, Vol. 5, pp. 184–189 (1966).
8. S. Sikka and M. Iqbal, Laminar heat transfer in a circular tube under solar conditions in space, *Int. J. Heat Mass Transfer* **19**, 975–983 (1970).
9. Ya. S. Kadaner, Yu. P. Rassadkin and E. L. Spektor, Heat transfer in laminar liquid flow through a pipe cooled by radiation, *Heat Transfer Soviet Res.* **3**(5), 182–188 (1971).
10. S. W. Churchill and H. H. S. Chu, Correlating equations for laminar and turbulent free convection from a horizontal cylinder, *Int. J. Heat Mass Transfer* **18**, 1049–1053 (1975).
11. E. M. Sparrow and S. V. Patankar, Relationships among boundary conditions and Nusselt numbers for thermally developed duct flows, *J. Heat Transfer* **99**, 483–485 (1977).

CONVECTION FORCEE DANS UN TUBE HORIZONTAL AVEC A L'EXTERIEUR CONVECTION NATURELLE NON LINEAIRE ET RAYONNEMENT

Résumé—Une étude de la convection thermique laminaire forcée dans un tube horizontal est menée dans le cas de pertes externes par convection naturelle et rayonnement. La différence de température entre la paroi du tube et l'ambiance varie longitudinalement. Puisque le coefficient de convection naturelle dépend de cette différence de température, il varie lui aussi le long du tube et on en tient compte d'une façon particulière. On trouve que tant que le nombre de Nusselt est généralement insensible à la variation du coefficient de convection externe, il n'existe pas un nombre de Nusselt constant de régime thermiquement établi. Ce rayonnement tend à diminuer le nombre de Nusselt du tube, mais le maximum d'effet est seulement proche de 10%. Les distributions de température de la paroi et du fluide sont généralement plus sensibles à la convection externe variable que n'est le nombre de Nusselt. Cette sensibilité diminue lorsque le rayonnement joue un rôle important dans la perte thermique.

ERZWUNGENE KONVEKTION IN EINEM HORIZONTALEN ROHR IN VERBINDUNG MIT NICHTLINEARER NATÜRLICHER KONVEKTION UND MIT STRAHLUNG AUF DER AUßENSEITE

Zusammenfassung—Der Wärmeübergang durch erzwungene Konvektion bei laminarer Strömung im waargerechten Rohr wurde untersucht, und zwar für den Fall, daß das strömende Fluid an die äußere Umgebung durch natürliche Konvektion und durch Strahlung Wärme abgibt. Die Temperaturdifferenz zwischen der Rohrwand und der Umgebung ändert sich entlang des Rohres. Da der Wärmeübergangskoeffizient der natürlichen Konvektion an der Außenseite von dieser Temperaturdifferenz abhängt, ändert auch er sich über die Rohrlänge. Die Berücksichtigung dieser Änderung ist ein besonderes Merkmal der Analyse. Es wurde gefunden, daß ein thermisch ausgebildetes Profil mit einer konstanten Nusselt-Zahl nicht existiert, obwohl die Nusselt-Zahl der Rohrströmung im allgemeinen doch unempfindlich gegenüber Veränderungen des äußeren Wärmeüberganges ist. Die Strahlung neigt dazu, die Nusselt-Zahl der Rohrströmung zu erniedrigen, wobei die maximale Auswirkung aber nur 10% beträgt. Die Verteilung der Wand- und der Mitteltemperatur hängen im allgemeinen stärker als die Nusselt-Zahl von veränderlicher äußerer Konvektion ab. Diese Abhängigkeit vermindert sich jedoch, wenn ein wesentlicher Teil der Wärmeverluste durch Strahlung verursacht wird.

ВЫНУЖДЕННАЯ КОНВЕКЦИЯ В ГОРИЗОНТАЛЬНОЙ ТРУБЕ В УСЛОВИЯХ НЕЛИНЕЙНОЙ ВНЕШНЕЙ ЕСТЕСТВЕННОЙ КОНВЕКЦИИ И ИЗЛУЧЕНИЯ

Аннотация — Проведен анализ ламинарного переноса тепла вынужденной конвекцией в горизонтальной трубе в случае, когда перенос тепла от потока жидкости в трубе во внешнюю окружающую среду происходит естественной конвекцией и излучением. Разность температур между стенкой трубы и окружающей средой изменялась по длине трубы. Поскольку коэффициент внешнего теплообмена естественной конвекцией зависит от разности температур, он также изменялся по длине трубы. Учет этого изменения составляет особенность рассмотренной задачи. Так как число Нуссельта для трубы почти не изменяется с изменением коэффициента внешнего конвективного теплообмена, то термически развитый режим с постоянным числом Нуссельта отсутствовал. Излучение понижало значение числа Нуссельта для трубы, но не более чем на 10%. Изменение величины внешнего конвективного потока тепла оказывало бóльшее влияние на профили температуры стенки и потока, чем на значения числа Нуссельта. Это влияние снижается с увеличением потерь тепла излучением.